Journal of Statistical Physics, Vol. 53, Nos. 3/4, 1988

Finite-Size Scaling in a Microcanonical Ensemble

Rashmi C. Desai,[1,2] Dieter W. Heermann,[1] and K. Binder[1]

Received May 3, 1988

The finite-size scaling technique is extended to a microcanonical ensemble. As an application, equilibrium magnetic properties of an $L \times L$ square lattice Ising model are computed using the microcanonical ensemble simulation technique of Creutz, and the results are analyzed using the microcanonical ensemble finite-size scaling. The computations were done on the multitransputer system of the Condensed Matter Theory Group at the University of Mainz.

KEY WORDS: Microcanonical ensemble; finite-size scaling; two-dimensional Ising model; transputers.

1. INTRODUCTION

Monte Carlo (MC) simulations[1] have been applied to a variety of systems and an impressive array of results have been obtained for many interesting physical properties. Many simulations are by, and largely done for, canonical ensemble systems and use pseudo-random number generators in an essential way. For many dynamic properties and some static properties, in the critical region, it is essential to have a high-quality random number generator (RNG). This is often costly in computational time. Some conventional RNGs also exhibit correlations, leading to subtle errors in the results. During the past 5 years, two different types of simulations have been introduced which use a deterministic approach in the configurational updating procedure and thereby avoid the use of an RNG during the main part of the simulation. These are the microcanonical ensemble (MCE) simulation method[2-5] due to Creutz and the Q2R algorithm.[6,7] In the

[1] Institut für Physik, Johannes-Gutenberg Universität Mainz, D-6500 Mainz, Federal Republic of Germany.

[2] Permanent address: Department of Physics, University of Toronto, Toronto, Ontario, MSS 1A7, Canada.

0022-4715/88/1100-0795$06.00/0

Q2R algorithm, only the total energy-conserving moves are made in the updating of spin configurations of a system, whereas in the MCE simulation method, one introduces one (or a small number of) demon(s) which acts as a movable heat bath. Each move of the local spins leaves the energy of the demons plus the system energy constrained to a constant. If the number of demons is small compared to the total number of degrees of freedom in the system, one has a simulation of the microcanonical ensemble. This idea can also be applied to the molecular dynamics (MD) method.[5]

Simulations are always done for finite systems; the extrapolation procedure to determine the behavior of physical properties in the thermodynamic limit has been dramatically improved by the recent advent of the finite-size scaling method.[8–11] Much of this literature is in the canonical ensemble framework, where temperature is the important independent variable, along with the scaled dimensionsless variable L/ξ, where L is the length related to the finite system under study, which has a correlation length ξ. Recent developments of the MCE and Q2R simulation techniques have made it timely to study once again aspects of thermodynamic and critical fluctuations in a microcanonical ensemble, for infinite and finite systems. As is well known, finite-size effects depend on the choice of statistical ensemble, although this does not matter in the thermodynamic limit.

The outline of the present work is as follows. The basic theoretical foundations are given in Section 2 (subdivided into more than a dozen subsections), where we first present a straightforward extension of thermodynamic scaling ideas to a microcanonical ensemble and then construct the scaling relations for both thermal and magnetic properties. These then naturally lead to the corresponding extension of finite-size scaling relations for a microcanonical ensemble, where the scaled variable L/ξ plays an important role. In the microcanonical ensemble, the intensive entropy density s and the magnetic field h are the natural choice for the pair of independent thermodynamic variables. In various scaling relations, the exponent α (related to the divergence of the heat capacity C_h near the critical point) figures prominently. We conclude Section 2 (Section 2.14) by considering the example of a 2D Ising system. Here C_h diverges logarithmically ($\alpha \sim 0$) and much is known analytically both for finite systems[12] and in the thermodynamic limit.[13,14] Also, there has been a detailed numerical study for its thermal and magnetic properties as a function of the system size in a canonical ensemble setting.[15] In Section 2.14, we propose how the finite-size scaling variable L/ξ can be practically implemented for the 2D Ising model.

In Section 3, we present the simulation results for the magnetic

properties of a square-lattice Ising system using the MCE simulation method; the simulations were done on a multitransputer system and programmed in OCCAM. While the minimal use of RNGs in the MCE simulation is its distinct advantage, we uncover some of its limitations for small-system simulations. The results show that even with a very modest computing effort, we can obtain interesting and useful results (like an old wine in a new bottle) for the 2D Ising model and at the same time explore the finite-size scaling technique for the microcanonical ensemble. We feel that this study should pave the way for the application of this microcanonical ensemble simulation method to phase transition problems in more complicated models of statistical mechanics, where no exact results are available for comparison.

2. FINITE-SIZE SCALING IN A MICROCANONICAL ENSEMBLE

2.1. Prelude

We consider magnetic systems with an Ising model as a prototype and measure various energies in units of a characteristic constant energy, like the near-neighbor interaction constant J_0; we also set the Boltzmann's constant to unity, e.g., temperature T is $(\beta J_0)^{-1}$ in more common notation. The four intensive variables T, s, m, and h and the four (extensive) thermodynamic potentials U, E, A, and G form the basis of any thermodynamic description of magnetic systems. (As far as possible, we use the notation from the textbook by Stanley[16]; the material relevant to this section may be found in Chapters 2 and 11 and Appendix C.) For a microcanonical ensemble, the enthalpy function $e(s, h) \equiv E/V$, for a system having the volume V, is a natural starting point in analyzing thermodynamic relations like $de = T\,ds - m\,dh$. Since $e = u - hm$, we see that for the special value $h = 0$, the internal energy U and the enthalpy E are equal. In the simulations using the MCE method, the total energy of the system plus the demon(s), $U + U_d$, is constrained to be a constant. For moderately large systems and a small number of demons, commonly used in practical simulations,[2–5] one has $U_d \ll U$ and the demon energy provides a measure of the width of the energy shell within which the system makes a "random" walk through its allowed configurations. The total number of the allowed states of the system $\Gamma(E)$ plays the role of the "partition function" in the microcanonical ensemble, and its logarithm, the entropy function S, is analogous to the free energy, or more precisely $(-A/T)$, in the canonical ensemble.

2.2. Enthalpy as a Homogeneous Function

In order to generalize the ideas of the scaling hypothesis used in critical phenomena and extend them to the finite-size scaling in a microcanonical ensemble, we follow a pedagogically simpler course of block spin transformations and homogeneous function postulates, even though the full renormalization group "machinery" can be used in principle. At the critical point, $T = T_c$, $h = 0$, $m = 0$, $s = s_c$, $e = e_c$, $u = u_c$, etc. One is interested in the behavior of various quantities in the vicinity of the critical point. Let $t = (T - T_c)/T_c$, $s^* = s - s_c$, $e^* = e - e_c$, etc. The enthalpy function and other thermodynamic potentials have a regular part and a nonanalytic part. Both parts are homogeneous functions of the arguments and the former is of degree one, reflecting the extensive property of the thermodynamic potentials. One may then write

$$e(s, h) = e_r(s, 0) + e^*(s^*, h) \tag{2.1}$$

such that at the critical point $e_r(s_c, 0) = e_c$ and $e^*(0, 0) = 0$. The regular part obeys

$$e_r(\lambda s, 0) = \lambda e_r(s, 0) \tag{2.2}$$

and we may postulate that

$$e^*(\lambda^{a_s} s^*, \lambda^{a_h} h) = \lambda e^*(s^*, h) \tag{2.3}$$

thereby introducing two exponents a_s and a_h characterizing the nonanalytic part of the enthalpy.

2.3. Temperature

The thermodynamic temperature in a microcanonical ensemble is obtained from the relation $de = T\,ds - m\,dh$, so that $T = (\partial e/\partial s)_h$. Its value T_c at $e = e_c$, $s = s_c$, is clearly nonzero, which requires us to write $de = de_r + de^*$ with $de_r = T_c\,ds$ and $de^* = (T - T_c)\,ds^* - m\,dh$, with the result $T_c t = (\partial e^*/\partial s^*)_h$ and $m = -(\partial e^*/\partial h)_{s^*}$. In the MCE simulation, the demon energy distribution reflects the temperature of the system through its mean.[2] In order to get the correct $(\partial e/\partial s)_h$, a proper sampling of the entropy fluctuations, i.e., an extensive scan of the system configurations, has to be made in the simulation.

2.4. Objective

Our objective is to express various critical exponents α, β, γ, δ in terms of the exponents a_s and a_h introduced in Eq. (2.3) and relate a_s and a_h to

the exponents η and ν, which reflect the single characteristic length near the critical point. We restrict our attention to systems where the critical exponents satisfy the hyperscaling relation and a single characteristic length applies. This, of course, is the correlation length ξ for an infinite system; for finite systems its role near T_c is transferred to L, the system size, and it is this aspect that introduces, through the finite-size scaling method, an additional scaling variable ξ/L in the scaling functions.

2.5. Exponent a_s

To this end, we differentiate Eq. (2.1) with respect to s^* ($s = s^* + s_c$) to get

$$\lambda \frac{\partial e_r(\lambda s^*, 0)}{\partial(\lambda s^*)} + \lambda^{a_s} \frac{\partial e^*(\lambda^{a_s} s^*, \lambda^{a_h} h)}{\partial(\lambda^{a_s} s^*)} = \lambda \frac{\partial e_r(s^*, 0)}{\partial s^*} + \lambda \frac{\partial e^*(s^*, h)}{\partial s^*}$$

The first term on both sides of this equation is equal to λT_c and we conclude that the function $t(s^*, h)$ is constrained by the relation

$$\lambda^{a_s - 1} t(\lambda^{a_s} s^*, \lambda^{a_h} h) = t(s^*, h) \tag{2.4}$$

in the critical region. Differentiating Eq. (2.1) once again with respect to s^* leads to similar scaling for the heat capacity C_h, since

$$(\partial^2 e/\partial s^2)_h = (\partial T/\partial s)_h = T/C_h$$

Near T_c, if the specific heat exponent α is positive, C_h is dominated by its diverging piece arising from the nonanalytic part e^*. One then can *neglect* the regular part to write

$$\left(\frac{\partial^2 e}{\partial s^2}\right)_h = \left(\frac{\partial^2 e}{\partial s^{*2}}\right)_h = \left[\left(\frac{\partial^2 e_r}{\partial s^{*2}}\right)_h + \left(\frac{\partial^2 e^*}{\partial s^{*2}}\right)_h\right] \approx \left(\frac{\partial^2 e^*}{\partial s^{*2}}\right)_h$$

which identifies $(\partial^2 e^*/\partial s^{*2})_h$ as T/C_h^* with C_h^* as the singular part behaving as $C_{h=0}^* |t|^{-\alpha}$, for zero field. By two differentiations of Eq. (2.3) with respect to s^*, we get the relation

$$C_h^*(s^*, h) = \frac{1 + t(s^*, h)}{1 + t(\lambda^{a_s} s^*, \lambda^{a_h} h)} C_h^*(\lambda^{a_s} s^*, \lambda^{a_h} h)\, \lambda^{-(2a_s - 1)} \tag{2.5a}$$

$$= \frac{1 + t(s^*, h)}{1 + \lambda^{1 - a_s} t(s^*, h)} C_h^*(\lambda^{a_s} s^*, \lambda^{a_h} h)\, \lambda^{-(2a_s - 1)} \tag{2.5b}$$

where we have used Eq. (2.4) to go from (2.5a) to (2.5b). It is now possible to extract the relation between the heat capacity exponent α and the scaling

exponent a_s, by setting $h=0$ and $\lambda=(s^*)^{-1/a_s}$ in Eqs. (2.4) and (2.5). For $\alpha \geqslant 0$, we anticipate $a_s \leqslant 1$ and neglect the terms $t(s^*, h)$ and $\lambda^{1-a_s} t(s^*, h)$ as small (compared to 1) in Eq. (2.5b) and get from Eq. (2.5b)

$$C_h^*(s^*, 0) = C_h^*(1, 0)(s^*)^{-(1-2a_s)/a_s}$$

and from Eq. (2.4)

$$t(s^*, 0) = t(1, 0)(s^*)^{(1-a_s)/a_s}$$

leading to the identification that

$$\alpha = \frac{1-2a_s}{1-a_s} \quad \text{and} \quad a_s = \frac{1-\alpha}{2-\alpha}, \qquad \alpha > 0 \tag{2.6}$$

2.6. Entropy, Temperature, C_h, e^*, and u^*

We also obtain as a result the singular behavior (for $\alpha > 0$)

$$C_h(s^*, 0) = C_h^*(1, 0)(s^*)^{-\alpha/(1-\alpha)} = \frac{C_h^*(1, 0)}{[t(1, 0)]^{-\alpha}} [t(s^*, 0)]^{-\alpha} \tag{2.7}$$

identifying the amplitude of the heat capacity and the behavior of the entropy as (for $\alpha > 0$)

$$s^* = [t(s^*, 0)/t(1, 0)]^{1-\alpha} \tag{2.8}$$

For a logarithmically divergent heat capacity, as is the case for the 2D Ising model, a naive setting of $\alpha = 0$ is not to be done. This case is discussed in Section 2.14. One may integrate Eq. (2.7) to obtain e^* as follows: since h is fixed at $h=0$, and $T=(\partial e/\partial s)_h$, we have

$$e = \int T \left(\frac{\partial s}{\partial T}\right)_h dT$$

from which we get

$$e^* = \int_{T_c}^{T} T \left(\frac{\partial s}{\partial T}\right)_h dT = T_c \int_0^t C_h \, dt \approx T_c \int_0^t C_h^* \, dt$$

and finally

$$e^*(s^*, 0) = \frac{T_c C_h^*(1, 0)\, t(1, 0)}{1-\alpha} s^* \tag{2.9a}$$

$$= \frac{T_c C_h^*(1, 0)}{1-\alpha} [t(1, 0)]^{\alpha} [t(s^*, 0)]^{1-\alpha} \tag{2.9b}$$

Note that, since $h=0$, $e^*(s^*, 0)=u^*(s^*, 0)$, and both are proportional to s^* or to $(t)^{1-\alpha}$.

2.7. $\Gamma(E)$ and the Demon Distribution away from Criticality

Near the critical point, the number of states of the system allowed by the constant-energy constraint in the microcanonical ensemble is related to s^*.

Since $\Gamma(E)=\exp(S)$, we have $\Gamma(E)/\Gamma(E_c)=\exp(S-S_c)=\exp(Vs^*)$. Thus, a calculation of s^*, e^*, and u^* also constitutes a calculation of $\Gamma(E)$ [relative to $\Gamma(E_c)$] in the neighborhood of the critical point. Away from the critical point, it is useful at this point to restate the standard results of a thermodynamic fluctuation theory. From $e(s, h)$, one may obtain in principle $s(e, h)$. Then, for $E \leqslant E_0 \leqslant E+\Delta E$, i.e., $e \leqslant e_0 \leqslant e_0+\Delta e$,

$$\begin{aligned} S(E_0, h, V) &= Vs(e_0, h) \\ &= V\left[s(e_0, 0)+\left(\frac{\partial s}{\partial e}\right)_h \Delta e+\frac{1}{2!}\left(\frac{\partial^2 s}{\partial s^2}\right)_h \Delta e^2+\cdots \right. \\ &\quad \left. +\left(\frac{\delta s}{\delta h}\right)_e h+\frac{1}{2!}\left(\frac{\delta^2 s}{\delta h^2}\right)_e h^2+\cdots \right] \\ &= V\left[s_0+\frac{1}{T}\Delta e+\frac{mh}{T}+\frac{1}{2C_h}\left(\frac{\Delta e}{T}\right)^2 \right. \\ &\quad \left. +\frac{1}{2}\left[\frac{\partial}{\partial h}\left(\frac{m}{T}\right)\right]_e h^2+\cdots \right] \end{aligned}$$

For the special choice $h=0$, $e=u$, and $\Delta e=\Delta u$, we get

$$S(U, V)=Vs(u)=V\left(s_0+\frac{1}{T}\Delta u-\frac{1}{2C_h T^2}\Delta u^2+\cdots \right)$$

The microcanonical ensemble distribution for the allowed states Γ is uniform and for one of the allowed configurations $\{\cdots\}$, its probability is $1/\Gamma$. (It is zero for disallowed states.) Thus, the probability for the MCE system to be in a configuration $\{\cdots\}$ is

$$\begin{aligned} P(\{\cdots\}) &= \frac{1}{\Gamma}=\exp(-S) \\ &= \exp\left[-V\left(s_0(u)+\frac{1}{T}\Delta u-\frac{1}{2C_h T^2}(\Delta u)^2+\cdots\right)\right], \qquad h=0 \end{aligned}$$

Since $U + U_d = \text{const}$, $V\Delta u = -\Delta U_d$ and we see that the demon energy distribution can be used to measure both the temperature T and the heat capacity C_h of the system.

2.8. Exponent a_h, Magnetization, and Susceptibility

We now return to Eq. (2.3) to determine the magnetic behavior and then relate the critical exponents β, γ, ∂ to a_h and a_s. Since $(\partial e^*/\partial h)_{s^*} = -m$ and $(\partial m/\partial h)_{s^*} = \chi_s$, we can differentiate Eq. (2.3) twice on h to obtain

$$\lambda^{a_h} m(\lambda^{a_s} s^*, \lambda^{a_h} h) = \lambda m(s^*, h) \tag{2.10}$$

$$\lambda^{2a_h} \chi_s(\lambda^{a_s} s^*, \lambda^{a_h} h) = \lambda \chi_s(s^*, h) \tag{2.11}$$

Again, we set $h = 0$ and $\lambda = (s^*)^{-1/a_s}$ in these two equations and get

$$m(s^*, 0) = m(1, 0)(s^*)^{(1-a_h)/a_s} \tag{2.12}$$

and

$$\chi_s(s^*, 0) = \chi_s(1, 0)(s^*)^{-(2a_h-1)/a_s} \tag{2.13}$$

In view of Eq. (2.8) and the definitions of the exponents β and γ, it is possible to identify

$$\beta = (1-\alpha)(1-a_h)/a_s = (2-\alpha)(1-a_h) \tag{2.14}$$

and

$$\gamma = (2-\alpha)(2a_h - 1) \tag{2.15}$$

From these, one can deduce that

$$a_h = (2-\alpha-\beta)/(2-\alpha) \tag{2.16}$$

and the scaling equality

$$\gamma = (2-\alpha-2\beta) \tag{2.17}$$

is satisfied. From Eqs. (2.6) and (2.16), we see that Eqs. (2.12) and (2.13) lead to entropy dependences of m and χ_s as $m(s^*) \sim (s^*)^{\beta/(1-\alpha)}$ and $\chi_s(s^*) \sim (s^*)^{-\gamma/(1-\alpha)}$ with the amplitudes as in Eqs. (2.12) and (2.13).

Also, for $h = 0$, $s^* \sim e^* \sim u^*$.

Next, by setting $s^* = 0$, $\lambda = (h)^{-1/a_h}$, in Eq. (2.10), we can identify the exponent δ as

$$\delta = a_h/(1-a_h) = (2-\alpha-\beta)/\beta \tag{2.18}$$

which leads to other known scaling relations involving the exponent δ (see Table 11.1 in ref. 16).

2.9. Block Spin Scaling, Correlation Length, and Correlation Function

In order to extend the above results, valid for infinite systems, to finite systems, it is natural to use the coarse graining of the microscopic Hamiltonian via the Kadanoff block spin transformation. Consider the nearest-neighbor Ising Hamiltonian in d dimensions,

$$\mathscr{H} = -J \sum_{\langle ll' \rangle} \sum S_l S_{l'} - h \sum_{l=1}^{N} S_l$$

where J, h, and $\mathscr{H}$ are measured in units of a characteristic energy J_0 and the lattice spacing is set to unity. Such a lattice is coarse-grained by constructing blocks of side L such that $\xi \gg L \gg 1$, ξ being the correlation length. The original N-spin Hamiltonian is then transformed to an n-block-spin Hamiltonian ($n = N/L^d$) with the block spin defined as

$$s_i = \frac{1}{\mathscr{L} L^d} \sum_{l \in i} S_l$$

Here $\mathscr{L}$ is an important scale parameter, yet to be determined. In the critical region, one assumes that all the spins within a block behave like Ising spins; since $L \ll \xi$, all the spins within a block are mostly either all up or all down. Thus, after the transformation, the Hamiltonian is still of the Ising form but with new renormalized values of the couplings, i.e., $\mathscr{H}(J, h) \to \mathscr{H}(\tilde{J}, \tilde{h})$.

Similarly, the (intensive) thermodynamic potentials such as the enthalpy function *per spin* are the *same* functions but of the new couplings:

$$ne^*(\tilde{s}^*, \tilde{h}) = nL^d e^*(s^*, h) \tag{2.19}$$

where the transformation $(J, h) \to (\tilde{J}, \tilde{h})$ can in principle also provide the new values $(s^*, h) \to (\tilde{s}^*, \tilde{h})$. Comparing to Eq. (2.3), however, one may anticipate the result of such an analysis:

$$\tilde{s}^* = L^{y'} s^* = L^{da_s} s^* \tag{2.20a}$$

and

$$\tilde{h} = L^x h = L^{da_h} h \tag{2.20b}$$

The transformation of the field term in the Ising Hamiltonian is quite straightforward and leads us to the evaluation of the scale factor $\mathscr{L}$

$$\mathscr{L} \sim L^{(x-d)} = L^{d(1-a_h)} \tag{2.21}$$

The transformation of the spin–spin correlation function in zero field

$$\Gamma(r, s^*) \equiv \langle (S_l - \langle S_l \rangle)(S_{l'} - \langle S_{l'} \rangle) \rangle$$

where $\langle \cdots \rangle$ is the average over a microcanonical ensemble, leads to the correlation function of block spins

$$\Gamma(\tilde{r}, \tilde{s}^*) \equiv \langle (s_i - \langle s_i \rangle)(s_j - \langle s_j \rangle) \rangle$$

such that

$$\Gamma(r, s^*) = \mathscr{L}^2 \Gamma(\tilde{r}, \tilde{s}^*)$$

where the factor $\mathscr{L}^2$ arises from the block spin definition

$$\mathscr{L} s_i = \frac{1}{L^d} \sum_{l \in i} S_l$$

and $\tilde{r} = r/L$. The entropy variable s^* is related to $\tilde{s}^*$ as $\tilde{s}^* = L^{y'} s^* = L^{da_s} s^*$ and $\mathscr{L}^2 = L^{2d(a_h - 1)}$. Thus, we get

$$\Gamma(r, s^*) = L^{2d(a_h - 1)} \Gamma(r/L, L^{da_s} s^*) \tag{2.22}$$

as a relation [analogous to Eqs. (2.4), (2.5), (2.10), (2.11)] for the correlation function. In a standard way, let us set $L = (s^*)^{-1/(da_s)}$ in Eq. (2.22) to get

$$L(r, s^*) = (s^*)^{2(1-a_h)/a_s} \Gamma(r/\xi, 1) \tag{2.23}$$

where we identify the correlation length ξ as the single length and infer $\xi \sim (s^*)^{-1/(da_s)}$, so that, using Eq. (2.6), we can write

$$\xi \sim (s^*)^{-\tilde{\nu}} \qquad \text{with } \tilde{\nu} = (2-\alpha)/d(1-\alpha) \tag{2.24}$$

as the behavior of the entropy dependence of the correlation length in the microcanonical ensemble. Since $s^* \sim t^{(1-\alpha)}$ and $\xi \sim t^{-\nu}$, we get $\nu = (2-\alpha)/d$, which is the well-known hyperscaling relation, indicating overall consistency in the argument. Next, we let $L = r$ in Eq. (2.22). Then

$$\begin{aligned} \Gamma(r, s^*) &= r^{2d(a_h - 1)} \Gamma(1, (r s^{*1/da_s})^{da_s}) \\ &\equiv r^{-(d-2+\eta)} \tilde{\Gamma}(r/\xi) \end{aligned} \tag{2.25}$$

where we have used the definition of the exponent η. Thus, we can identify

$$(d-2+\eta)=2d(1-a_h) \tag{2.25a}$$

By using Eq. (2.16) for a_h in Eq. (2.25) and other relations previously obtained, we can get the known scaling relations involving η as

$$(d-2+\eta)=2d\beta/(2-\alpha)=d(2-\alpha-\gamma)/(2-\alpha)=2d/(\delta+1)=2\beta/\nu \tag{2.26}$$

2.10. Scaled Variables for Infinite Systems

In Eqs. (2.4), (2.5), (2.10), (2.11), and (2.22) we derived the scaling of T, C_h, m, χ, and $\Gamma(r, s^*)$, respectively. We have utilized them to obtain various scaling relations among the critical exponents and have also identified the values of the exponents a_s and a_h, respectively, in Eqs. (2.6) and (2.16). For the sake of completeness, let us also note that from Eq. (2.10), by setting $\lambda=|s^*|^{-1/a_s}$ and using Eqs. (2.6) and (2.16), we can get the scaled form of the magnetic equation of state for an infinite system in a microcanonical ensemble as

$$m(s^*, h)=|s^*|^{\beta/(1-\alpha)}\tilde{m}\left(\frac{s^*}{|s^*|}, \frac{h}{|s^*|^{\beta\delta/(1-\alpha)}}\right) \tag{2.27}$$

from which the scaled magnetization and scaled magnetic field emerge naturally as

$$\tilde{\tilde{m}}=|s^*|^{-\beta/(1-\alpha)}m(s^*, h) \tag{2.28a}$$

$$\tilde{\tilde{h}}=h\,|s^*|^{-\beta\delta/(1-\alpha)} \tag{2.28b}$$

These are consistent with the results of a similar analysis in a canonical ensemble due to Eq. (2.8).

2.11. Finite Systems and the Probability Distribution Function (PDF) for the Order Parameter

The above results generalize in a straightforward way to finite systems. We follow the analysis of ref. 10. For an Ising Hamiltonian

$$\mathscr{H}=-J\sum_{\langle ll'\rangle}\sum S_l S_{l'}-h\sum_l S_l$$

the microcanonical ensemble distribution is

$$P_{\mathrm{MC}}(\{S_l\})=\delta(E_0-\mathscr{H}[\{S_l\}])\Big/\sum_{E\leqslant E_0\leqslant E+\Delta E}\delta(E_0-\mathscr{H}[\{S_l\}]) \tag{2.29}$$

where the enthalpy E_0 is constrained to be within a narrow range between E and $E+\Delta E$, the numerator is a Kronecker delta of the argument shown,

and the denominator is simply the total number of allowed states of the system $\Gamma(E)$ as discussed in Section 2.7. In practical terms, $P_{\mathrm{MC}}(\{S_l\})$ is simply a uniform distribution with a value $1/\Gamma(E)$ for any allowed configuration $\{S_l\}$ and zero for the disallowed ones. In ref. 10, the role of the reduced distribution for one block spin s_i has been discussed in detail. Here we consider the case of the entire system of volume $L^d \equiv N$ as one block with periodic boundary condition and define the appropriate reduced distribution as

$$P_L(\bar{\sigma}, h) = \left\langle \delta\left(\sum_{l=1}^{N} S_l - N\bar{\sigma}\right)\right\rangle \tag{2.30}$$

where $\langle \cdots \rangle$ is an average over the distribution P_{MC}. For a similar distribution, but appropriate to a canonical ensemble, of a finite Ising square lattice, a number of results are given by McCoy and Wu and discussed in detail in Chapter XIII of ref. 14 [see particularly Eqs. (1.8), (3.4), and (3.23) and Fig. 13.1]. These results, obtained with a saddle point approximation, show that (1) for $T < T_c$, $P_L(\bar{\sigma}, 0)$ is a sum of two displaced Gaussians (displaced around the equilibrium magnetization values), (2) for $T > T_c$ it is a single Gaussian centered zero, and (3) at $T = T_c$, it is a very sharply peaked function of the form $A \exp(-B\,|\bar{\sigma}|^{\delta+1})$, where $\delta = 15$, and A and B are functions of temperature, N, δ, and K [at T_c, the magnetization behaves like $m(T_c, h) \sim K\,\mathrm{sgn}(h)\,|h|^{1/\delta}$, which defines K]. In general, reduced distributions such as $P_L(\bar{\sigma}, \mathrm{h})$ are difficult to obtain analytically, as illustrated in ref. 14 for the Ising square lattice. It is therefore useful to *assume* that close to T_c, $P_L(\bar{\sigma}, h)$ satisfies a finite-size scaling ansatz, as $L \to \infty$,

$$P_L(\bar{\sigma}, h) = L^{\beta/\nu}\frac{a}{C_0}\tilde{P}\left(a\bar{\sigma}L^{\beta/\nu}, \frac{L}{\xi}, a'hL^{\beta\delta/\nu}\right) \tag{2.31}$$

Here a, a' are (nonuniversal) scale factors, while $\tilde{P}$ is a universal function of its arguments, and the constant C_0 ensures proper normalization of the total probability being unity. In postulating this form for $P_L(\bar{\sigma}, h)$, we have used its general properties as discussed in ref. 10 and assumed that they are ensemble independent. In most of what follows, we shall restrict ourselves to $h = 0$ and denote $P_L(\bar{\sigma}, 0)$ by $P_L(\bar{\sigma})$.

2.12. Moments of the PDF

We define the moments of the PDF $P_L(\bar{\sigma})$ as

$$\langle \bar{\sigma}^k \rangle_L \equiv \int_{-\infty}^{\infty} d\bar{\sigma}\, \bar{\sigma}^k P_L(\bar{\sigma}) \tag{2.32}$$

$$= L^{-k\beta/\nu}(a^k C_0)^{-1} \int_{-\infty}^{\infty} dz\, z^k \tilde{P}(z, L/\xi) \tag{2.32a}$$

where the integral, to be denoted by $f_k(L/\xi)$, is a universal function of L/ξ for each value of k. P_L is an even function of $\bar{\sigma}$ and thus all the odd moments vanish. The zero-field magnetization is $\langle|\bar{\sigma}|\rangle_L$ and can be related to $P_L(\bar{\sigma})$ as

$$\begin{aligned} m = \langle|\bar{\sigma}|\rangle_L &= \int_0^\infty d\bar{\sigma}\, \bar{\sigma} P_L(\bar{\sigma}) \\ &= L^{-\beta/\nu}(aC_0)^{-1} \int_0^\infty dz\, z\tilde{P}(z, L/\xi) \\ &\equiv L^{-\beta/\nu}\tilde{\tilde{m}}(L/\xi) \end{aligned} \tag{2.33}$$

which leads to a finite-size scaling ansatz for the (spontaneous) magnetization

$$m(s^*, L)\, L^{\beta/\nu} = \tilde{\tilde{m}}(L/\xi) = \tilde{m}_1(L(s^*)^{\tilde{\nu}}) \tag{2.34}$$

This form is seen to be consistent with Eqs. (2.28a) and (2.24), since from these equations, we get

$$m\,|s^*|^{-\beta/(1-\alpha)} \sim m\xi^{\beta/(1-\alpha)\tilde{\nu}} \sim m\xi^{\beta/\nu} \sim mL^{\beta/\nu}$$

for finite systems. Similarly, the consideration of the second moment $\langle\bar{\sigma}^2\rangle_L$ leads to the finite-size scaling ansatz for the susceptibility as

$$\begin{aligned} \chi_s' &= L^d[\langle\bar{\sigma}^2\rangle_L - \langle|\bar{\sigma}|\rangle_L^2] \\ &= L^d\left[L^{-2\beta/\nu}\frac{f_2(L/\xi)}{a^2C_0} - L^{-2\beta/\nu}\tilde{\tilde{m}}\left(\frac{L}{\xi}\right)\right] \\ &= L^{d-2\beta/\nu}\tilde{\tilde{\chi}}_s(L/\xi) \\ &\equiv L^{\gamma/\nu}\tilde{\tilde{\chi}}_s(L/\xi) \end{aligned}$$

Thus,

$$\chi_s'(s^*, L)\, L^{-\gamma/\nu} = \tilde{\tilde{\chi}}_s(L/\xi) = \tilde{\chi}_{s_1}(L(s^*)^{\tilde{\nu}}) \tag{2.35}$$

Note that χ_s' tends to the bulk susceptibility for $L \to \infty$ only in the ordered phase; in the disordered phase, the proper definition rather is $\chi_s = L^d\langle\bar{\sigma}^2\rangle_L$, which has the same scaling structure. Also, the cumulant function $U_L \equiv 1 - \langle\bar{\sigma}^4\rangle_L/3\langle\bar{\sigma}^2\rangle_L^2$ is a universal function of the scaling variable $(L/\xi) \equiv (L/\xi_0)(s^*)^{\tilde{\nu}} \sim L(s^*)^{\tilde{\nu}}$, i.e., $U_L(s^*) \equiv U(L/\xi)$.

2.13. The Scaled Variable L/ξ

Equations (2.34) and (2.35), as well as the universal cumulant function $U(L/\xi)$, show that in zero-magnetic-field-limit, m, χ_s, and U_L can be scaled and expressed as functions of a single variable (L/ξ). This variable can be expressed in terms of the intensive entropy s^* as done above, in terms of the temperature t, using Eq. (2.8), or in terms of the intensive enthalpy e^*, using Eq. (2.9a). For $h=0$, $e^*=u^*$. We get

$$\frac{L}{\xi}=\frac{L}{\xi_0}(s^*)^{\tilde{\nu}}=\frac{L}{\tilde{\xi}_0}\left[\frac{t(s^*,0)}{t(1,0)}\right]^{\nu}=\frac{L}{\xi_0}t^{\nu}$$
$$=\frac{L}{\tilde{\xi}_0}\left[\frac{1-\alpha}{T_c C_h^*(1,0)\,t(1,0)}\right]^{\tilde{\nu}}(e^*)^{\tilde{\nu}}=\frac{L}{\tilde{\tilde{\xi}}_0}(e^*)^{\tilde{\nu}}$$

where $\nu=(2-\alpha)/d$, $\tilde{\nu}=\nu/(1-\alpha)$, and ξ_0, $\tilde{\xi}_0$, $\tilde{\tilde{\xi}}_0$ are the amplitudes of the correlation length in the three representations. In the simulations using the MCE technique, one has the system size L and the total energy $U+U_d$ prescribed and during the course of the simulation, one can determine both the mean system energy and the mean demon energy. For the simulations with one demon, since $L^d \gg 1$ in most instances, the intensive system energy u is practially the same as its initial value when the demon energy is chosen to be zero. Since the value of u at the critical point u_c is either known or is determined in the course of simulations, it is straightforward to construct the scaled variable $L(u^*)^{-\tilde{\nu}}$ in practice. For the case of a 2D Ising system, some of the results of this section have to be refined due to the logarithmic divergence of C_h instead of the $t^{-\alpha}$-type behavior.

2.14. The Square Lattice Ising Model and the Scaled Variable L/ξ

For the 2D Ising model, $\beta=1/8$, $\gamma=7/4$, and $\nu=1$. Due to the logarithmic heat capacity, which implies $\alpha=0$, naively $\tilde{\nu}=\nu/(1-\alpha)$ implies $\tilde{\nu}\sim\nu=1$. The scaled variable L/ξ in the canonical ensemble becomes $L/\xi=(L/\xi_0)\,t^{\nu}\sim Lt$, and would become $\sim Lu^*=L(u-u_c)$. This, however, is an inappropriate scaling variable for the 2D Ising model. A renormalization group analysis, including corrections to scaling,[17] is appropriate for a microcanonical ensemble. Here we take, however, an empirical approach: In place of Eq. (2.7), where we had $C_h\sim t^{-\alpha}$, we know that for the 2D Ising model [see Eq. (5.3.58), p. 95, ref. 14] C_h is of the form

$$C_h^*(t,0)=A_1-A_2\ln|t| \tag{2.36}$$

From this, using $e^* \simeq T_c \int_0^t C_h^* \, dt$, we get

$$e^*(t, 0) = T_c[(A_1 + A_2)\, t - A_2 t \ln t], \qquad t > 0 \tag{2.37}$$

which is not of the form of Eq. (2.9b) with $\alpha = 0$. Similarly, by using $s^* \simeq \int_0^t dt\, C_h^*/(1+t)$, one can show that Eq. (2.36) implies

$$s^*(t, 0) = A_1 \ln(1+t) - A_2(\ln t)[\ln(1+t)] - A_2 \sum_{n=0}^{\infty} \frac{(-t)^{n+1}}{(n+1)^2} \tag{2.38}$$

which has a singular part [for small t, $\ln(1+t) \approx t$] of the form $-A_2 t \ln t$; this again is not of the form of Eq. (2.8) with $\alpha = 0$. Similar differences in other quantities, such as ξ [Eq. (2.24)], where the exponents α and a_s enter in the analysis above, are expected. The quantities related to a_h seem to be unaffected. Our objective is to construct a scaled variable L/ξ as a function of $u^* = e^*$. This we do by noting the analytical results of Ferdinand and Fisher[12] (FF) for the Ising square lattice systems. For an $L \times L$ system, the intensive internal energy $u(L)$ is given by FF and is of the form [Eqs. (4.13) and (4.15) of ref. 12]

$$u(L, t) = +u_c(L) + \frac{4}{\pi} \tau \frac{\ln L}{L} + \frac{A(\tau)}{L} \tag{2.39}$$

where $\tau = Lt$, which is then seen to be an inappropriate scaling variable for u in a canonical ensemble. In Eq. (2.39), $A(\tau)$ is of the form $\tau \ln |\tau|$ and is thus zero at $\tau = 0$; the critical value $u_c(L)$ for the internal energy of a finite $L \times L$ Ising lattice is computed [Eq. (4.15), ref. 12] to be, in the canonical ensemble,

$$u_c(L) = u_c - 0.622440/L \tag{2.40}$$

where $u_c = -\sqrt{2}$ is the infinite lattice value at T_c, which is also known: $T_c = 2.269185\ldots$. From Eq. (2.39), we can write

$$\frac{u(L, T) - u_c(L)}{t} = \frac{4}{\pi} \ln L + \frac{A(\tau)}{\tau} \tag{2.41}$$

The first term on the right-hand side renders the left-hand side a function of both variables L and t instead of a single scaled variable τ; but if we subtract from the left-hand side its value at some noncritical temperature T_0 which is far away from T_c, we remove the unscalable term $(4/\pi) \ln L$, which depends only on L. Thus, we have the combination $\tilde{\tilde{u}}$ defined as

$$\begin{aligned} \tilde{\tilde{u}} &\equiv \frac{u(L, t) - u_c(L)}{T - T_c} - \frac{u(L, t_0) - u_c(L)}{T_0 - T_c} \\ &= \frac{1}{T_c}\left(\frac{A(\tau)}{\tau} - \frac{A(\tau_0)}{\tau_0}\right) \sim \frac{1}{T_c} \ln \frac{|\tau|}{|\tau_0|} \end{aligned} \tag{2.42}$$

such that it is a function of the scaled variable $\tau \equiv Lt \sim L/\xi$. At the critical point $\tau = 0$, $\tilde{u}$ defined above becomes infinite and therefore it is useful to use $(1/\tilde{u})$, which is like (ξ/L), as the scaled variable in the energy representation of the microcanonical ensemble for a system with a logarithmically diverging heat capacity. Although we have obtained these results from a discussion in the framework of the canonical ensemble, we suggest that they can be carried over into the microcanonical ensemble as well: the general scaling structure should have the same form there, although the explicit scaling functions certainly differ from those of the canonical ensemble, where t is eliminated in favor of $\tilde{u}$ by means of Eq. (2.42).

2.15. The Case of Negative Specific Heat Exponents

So far, we have assumed that the specific heat diverges at the phase transition. However, it is well known that for some cases of practical interest (such as the three-dimensional Heisenberg model) the specific heat exponent α is negative. Then, the regular part of the specific heat must not be neglected near the critical point in comparison with the singular one, which actually vanishes there. Thus, we have

$$\left(\frac{\partial^2 e}{\partial s^{*2}}\right)_h \equiv \frac{T}{C_h} = \left(\frac{\partial^2 e_r}{\partial s^{*2}}\right)_h + \left(\frac{\partial^2 e^*}{\partial s^{*2}}\right)_h = \frac{T}{C_h^r + C_h^*} \tag{2.43}$$

Writing $e_r = T_c s^* + \frac{1}{2} T_c \Gamma s^{*2} + \cdots$, where Γ is some constant, we find, instead of Eq. (2.4), using Eq. (2.3),

$$\begin{aligned} T = T_c(1+t) &= \left(\frac{\partial e_r}{\partial s^*}\right)_h + \left(\frac{\partial e^*}{\partial s^*}\right)_h \\ &= T_c(1 + \Gamma s^*) + \frac{1}{\lambda}\frac{\partial}{\partial s^*} e^*(\lambda^{a_s} s^*, \lambda^{a_h} h) \end{aligned} \tag{2.44a}$$

and hence

$$t = t_r + t^*(s^*, h) = \Gamma s^* + \lambda^{a_s - 1} t^*(\lambda^{a_s} s^*, \lambda^{a_h} h) \tag{2.44b}$$

replaces Eq. (2.4), with $t^* = (1/T_c)(\partial e^*/\partial s^*)_h$. Similarly, Eq. (2.43) yields, with the help of Eq. (2.3),

$$\left(\frac{\partial^2 e}{\partial s^{*2}}\right)_h = T_c \left[\Gamma + \lambda^{(2a_s - 1)} \frac{\partial t^*}{\partial s^*}(\lambda^{a_s} s^*, \lambda^{a_h} h)\right] \tag{2.45}$$

and hence the specific heat becomes

$$C_h = \frac{T}{T_c}\left[\Gamma + \lambda^{(2a_s-1)}\frac{\partial t^*}{\partial s^*}(\lambda^{a_s}s^*, \lambda^{a_h}h)\right]^{-1}$$

$$\approx \Gamma^{-1} - \Gamma^{-2}\lambda^{(2a_s-1)}\frac{\partial t^*}{\partial s^*}(\lambda^{a_s}s^*, \lambda^{a_h}h) \tag{2.46}$$

As a result, we can identify the regular and singular parts of the specific heat as

$$C_h^r = \Gamma^{-1}, \qquad C_h^*(s^*, h) = \lambda^{(2a_s-1)}C_h^*(\lambda^{a_s}s^*, 2^{a_h}h) \tag{2.47}$$

but note that the sign of the scaling power of λ in front of C_h^* on the rhs of this equation is just the reverse of Eq. (2.5). As expected, the singular term in Eq. (2.47) has the same structure as Eq. (2.5); this implies

$$C_h^*(s^*, 0) = C_h^*(1, 0)(s^*)^{(1-2a_s)/a_s} \tag{2.48a}$$

$$t(s^*, 0) = \Gamma s^* + t^*(1, 0)\, s^{*(1-a_s)/a_s} \xrightarrow[s^*\to 0]{} \Gamma s^* \tag{2.48b}$$

Since $\alpha < 0$ corresponds to $a_s < 1/2$, actually the first term in Eq. (2.48b) is the dominant one.

From Eqs. (2.48a), (2.48b) it follows Eq. (2.6) is replaced by

$$\alpha = -(1-2a_s)/a_s, \qquad a_s = 1/(2-\alpha) \tag{2.49}$$

and the specific heat expressed as a function of temperature becomes

$$C_h = \Gamma^{-1} + C_h^*(1, 0)(t/\Gamma)^{-\alpha}, \qquad \alpha < 0 \tag{2.50}$$

instead of Eq. (2.7), and similarly Eq. (2.8) is replaced by

$$s^* = \Gamma^{-1}[t - t^*(1, 0)(t/\Gamma)^{(1-\alpha)}] \tag{2.51}$$

At the same time, a linear term in t or in s^* appears in the energy as well,

$$e - e_c = T_c\int_0^t C_h\, dt = T_c\left[\Gamma^{-1}t + C_h^*(1, 0)\frac{t^{1-\alpha}}{1-\alpha}\Gamma^{\alpha}\right] \tag{2.52a}$$

or

$$e - e_c = T_c\left\{s^* + \left[C_h^*(1, 0)\frac{\Gamma}{1-\alpha} + \frac{t^*(1, 0)}{\Gamma}\right]s^{*1-\alpha}\right\} \tag{2.52b}$$

where only the leading-order terms have been kept. Thus Eqs. (2.52a) and (2.52b) replace Eqs. (9a) and (9b).

Since Eq. (2.49) is the same scaling power that appears for the temperature in the canonical ensemble, as it must be, since asymptotically t and s^* are linearly related [Eq. (2.48b)], scaling relations such as Eq. (2.17) are again satisfied.

3. AN APPLICATION TO THE 2D ISING MODEL

In this section we describe a simulation of the square-lattice Ising model using the MCE technique,[2] present the results obtained for finite $L \times L$ lattice with $L = 8$, 10, 20, 25, 30, and 60, and present the finite-size scaling analysis of these results using the formulation described in Section 2.

3.1. Simulation of the 2D Ising Model Using Transputers

The MCE simulation of an $L \times L$ square lattice Ising system was done using a multitransputer system made up of four transputer chips on two boards, installed in an IBM PC-AT. The Inmos transputer chip is a 32-bit CMOS microprocessor which is specifically designed to support parallel processing in large networks of interconnected processors. We have implemented the MCE algorithm[5] in OCCAM at the simplest and most rudimentary level. The four-transputer system is configured such that input–output between it and the PC-AT occurs through one of the four (host) chips and the other three (slaves) used in parallel to generate three simulations simultaneously. For a detailed discussion see ref. 18. Without any sophistication (e.g., multispin coding) of complex programming, we are able to obtain a speed of about 5.6 μsec per spin flip. In the MCE simulation, we use one demon which visits the $L \times L$ lattice (with periodic boundary conditions) sites sequentially. At each site, the local near-neighbor spin configuration is checked and the spin is flipped deterministically, as is the energy change of the system given to the demon, provided that in the process the demon energy does not become negative. Initially, the demon energy is zero and the system energy is the initial total prescribed energy. One "Monte Carlo step" (unit of time) is defined to be the time taken by the demon to visit all the L^2 sites of the lattice once. Typically, for a given value of the system parameters (L, U), one generates configurations for $(m+n)$ Monte Carlo steps, discards the first m steps, and constructs averages for various physical properties from the remaining n configurations, skipping every $(n_0 - 1)$ steps; i.e., one has averages over n/n_0 Monte Carlo steps. In our simulations typically $m = 1000$, $n_0 = L$, and $n/n_0 = 5000$, with selected data points with $n_0 = L^2$ and $n/n_0 = 10{,}000$. Without a great deal of effort in creating a sophisticated program, the four-transputer system took an overnight run of approximately 36,000 sec to

generate a typical set of $3(L, U)$ data points with $L = 60$, $m = 10{,}000$, $n_0 = L$, and $n/n_0 = 10{,}000$. Our purpose here is not to show that the known analytic results for the 2D Ising model can be reproduced with great accuracy, but to demonstrate the use of a multitransputer system (we have barely begun to tap its potential!) and apply the finite-size scaling technique to the MCE simulation results.

A study of the dynamic correlations—time-dependent magnetization autocorrelation function—using the same program and the transputer configuration described above is reported elsewhere[18]; there, using the finite-size scaling technique, we have obtained (1) the scaled magnetization autocorrelation function at zero time, which is related to the susceptibility χ, (2) the dynamic critical exponent z for the 2D Ising model in equilibrium, and (3) the scaled relaxation time as a function of the scaled temperature τ. Here, in the next subsection, we describe the results for the static magnetic properties of the 2D Ising model—magnetization m, susceptibility χ, and the cumulant U, using the MCE simulation.

3.2. Results of the MCE Simulation

For the Ising square lattice ($L \times L$), the ground-state energy is $-2JL^2$ and the disordered state energy is 0. Thus, the intensive energy u measured

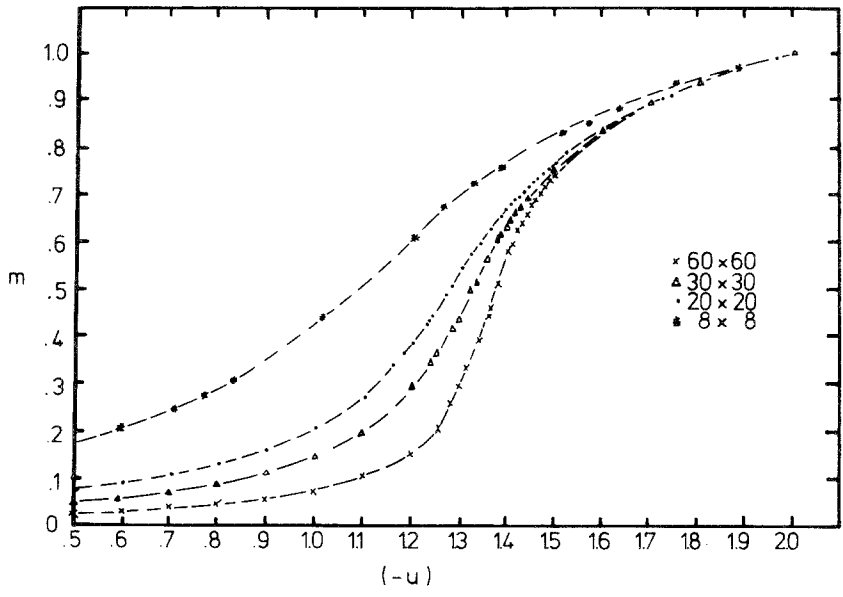

Fig. 1. Magnetization m as a function of the intensive internal energy u. Note $-u$ on the horizontal scale. (*) $L = 8$, (○) $L = 20$, (△) $L = 30$, (×) $L = 60$.

in units of J varies between -2 and 0. In Fig. 1, we show the magnetization m as a function of $(-u)$ for $L=8$, 20, 30, and 60; in Fig. 2 we display the susceptibility χ as a function of $(-u)$ for $L=8$, 10, 20, 25, 30, and 60. As expected, the magnetization is smooth and continuous through the critical point energy $-u_c = +\sqrt{2}$, since we have finite systems which do not have any phase transition, in principle. The behavior of the susceptibility also shows peaks with finite maximum values $\chi_{\max}$. It is seen that both $\chi_{\max}$ and the peak positions $u_{\max}$ depend on the system size. Thus, the effective critical point occurs at an L-dependent $u_{\max}(L)$. In Fig. 3, we show these dependences on L: Fig. 3a shows $u_{\max}(L)$ and Fig. 3b shows $\chi_{\max}(L)$. Within the error bars, $u_{\max}$ is a linear function of $L^{-1/\nu} \equiv 1/L$ and extrapolates to the expected value of $-\sqrt{2}$. From Fig. 3b, which is a double logarithmic plot of $\chi_{\max}$ versus L, we find a slope of 1.8 ± 0.1, whereas the expected value γ/ν is 1.75. By using the relation $T(u)$

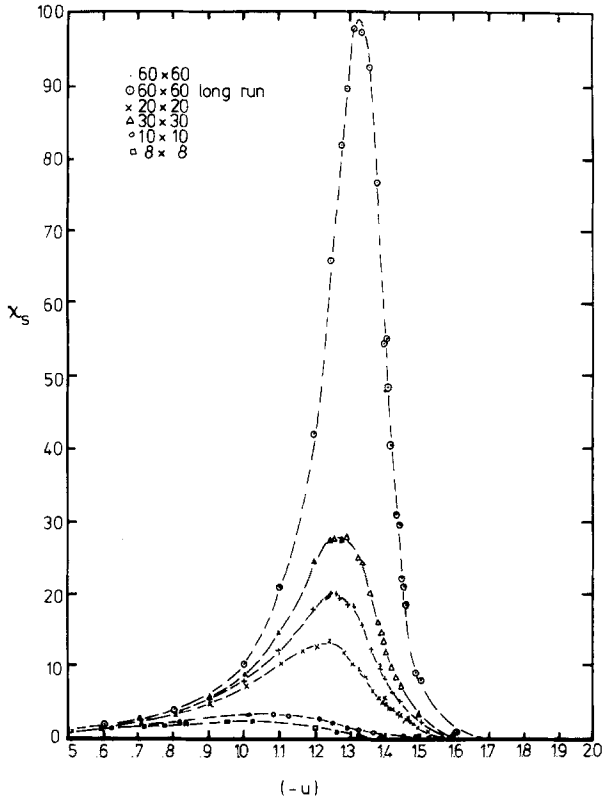

Fig. 2. Susceptibility χ_s as a function of $-u$ for various values of the system size L: (□) 8, (○) 10, (×) 20, (+) 25, (△) 30, and (⊙) = 60.

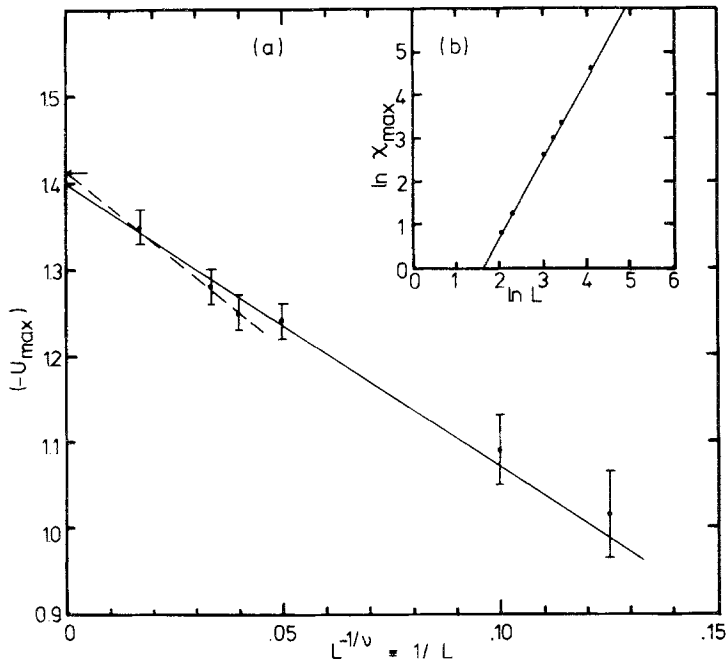

Fig. 3. (a) $-u_{max}$ versus $L^{-1/\nu} \equiv 1/L$; see text for details; $-u_c = \sqrt{2}$; (b) $\ln \chi_{max}$ versus $\ln L$. The slope of the line is 1.8 ± 0.1; see text for details.

(refs. 13 and 14), we estimate that the effective temperature (for finite systems) $T_c^{\chi}(L)$ is of the form

$$T_c^{\chi}(L) = T_c\left(1 + \frac{1.02 \pm 0.09}{L}\right)$$

It compares favorably with earlier numerical work of Landau.[15] It is also to be contrasted with Eq. (2.40), which is the analogous result for the heat capacity in the canonical ensemble.

3.3. Critique of the MCE Simulation Technique

During the MCE simulation, the demon energy distribution gives the system temperature.[2] In our study of dynamic correlations,[18] we have found that in order to reproduce the analytically known[13,14] temperature $T(u)$ accurately to four significant figures, one needs to average over about 2.5 million configurations for $L \geqslant 20$. For smaller systems, even this is not sufficient. In the results reported here, we use the analytic relation for $T(u)$

to obtain the temperature from the system energy u. Even though the system energy is an independent variable, its value can be prescribed only within the fluctuation $\langle u_d \rangle \equiv \langle U_d \rangle / L^2$. For small systems (e.g., $L = 8$), $\langle u_d \rangle$ can be a significant fraction of u. For $L \geqslant 20$, this is not a significant impediment in performing the simulation. The advantage of using the finite-size scaling technique is that one need not do simulations on very large systems to study fluctuations and correlations. The above remarks show that in the MCE simulations, the data reliability is impaired if the systems simulated are too small. An advantage of the MCE simulation technique is its computational efficiency and speed, since the use of RNGs is (almost) eliminated. For large systems, near the critical point, another general disadvantage for all simulations is the long dynamic correlations[18] present in the system. This requires that $n_0 \sim L^z$, where z is the dynamic critical exponent. Our data for $L = 60$ with $n_0 \sim L$ show a systematic trend indicating an insufficient statistical averaging. In doing the finite-size scaling, we have used the data with $L = 20$, 25, and 30.

Another problem which matters for very large lattices in principle, but for small enough lattices in practice, is the fact that due to the perfect deterministic character of the algorithm, there will be a finite (albeit very large) recurrence time where the initial spin configuration occurs again and at the same time the demon energy is zero, and from there on the simulation reproduces itself. Increasing the observation time beyond the recurrence time would make no sense, which also implies that the "statistical" error cannot be made arbitrarily small, and the algorithm as it stands perhaps suffers also from a lack of ergodicity (it is not clear that within the recurrence time all states consistent with a chosen total energy are actually reached).

An obvious approach to remedy this situation would be to introduce another element of stochasticity into the algorithm: e.g., after every n' step (with $n_0 \ll n' \ll n$) we move the demon not to the next lattice site as usually done, but to a randomly chosen lattice site anywhere in the system. This procedure would not affect the efficiency of the algorithm much. In practice, we have not yet implemented this procedure (or other alternatives to eliminate this problem), because it is clear that the recurrence time is much larger than the observation times used here for the values of L and system energies studied.

3.4. Finite-Size Scaling Analysis of the MCE Simulation Data

We apply the results of Section 2 [Eqs. (2.42), (2.35), (2.34)] to the results discussed in Sections 3.2 and 3.3. In Fig. 4, we show the cumulant U_L as a function of T for $L = 8$, 10, 20, 25, and 30. Here we use the exactly

known[13] relation between u and T appropriate for an infinite lattice to transform from dependences as a function of u to dependences as a function of T. In principle, there is also a finite-size effect in the actual system temperature $T = T(u, L)$, which follows from the demon energy distribution, but in practice this size effect hardly exceeds the statistical error[18] and hence is disregarded here. We expect[10] a common intersection point at T_c. The data for $L = 20$, 25, and 30 do show such a crossing around $T \approx 2.27$, which is quite close to $T_c = 2.269185...$. The value of the fixed point cumulant U^*_{MCE} (in the microcanonical ensemble) is about 0.645 ± 0.01, where the error is simply an estimate of the scatter of the data

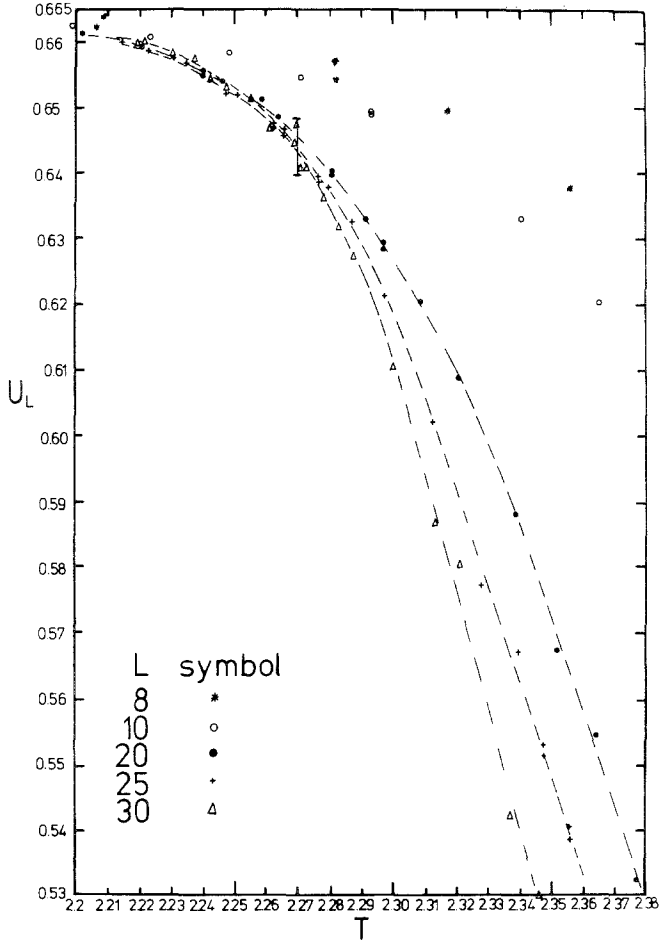

Fig. 4. The cumulant function U_L as a function of temperature T for $L = (*)$ 8, $(\circ)$ 10, $(\bullet)$ 20, $(+)$ 25, and $(\triangle)$ 30. See Section 3.3 for discussion on the data for $L = 8$ and 10.

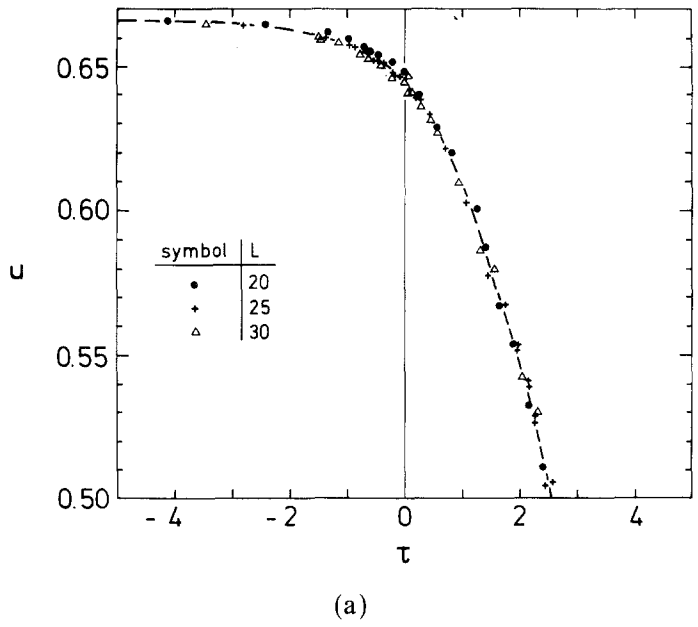

(a)

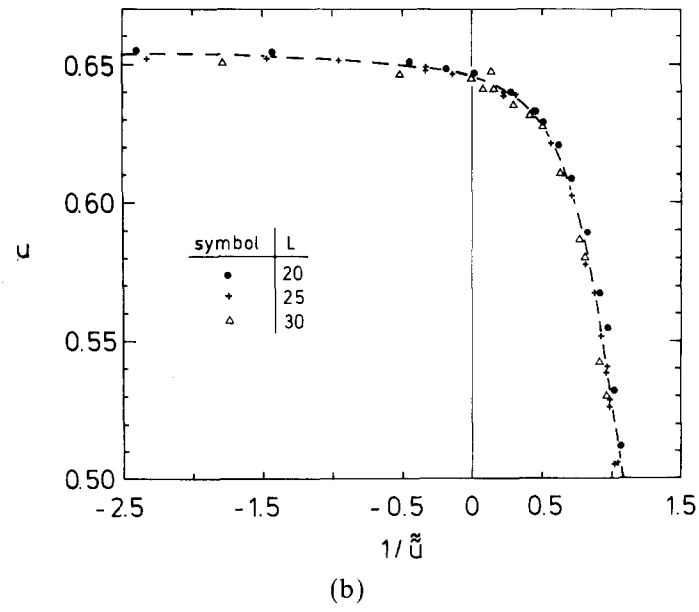

(b)

Fig. 5. (a) U as a function of τ, the scaled temperature. (b) U as a function of $1/\tilde{u}$ the reciprocal of scaled internal energy. See Eq. (2.42) and Section 2.14 for discussion of $\tilde{u}$ and τ.

points; this value is higher than other previous estimates of U^*_{CE} (in the canonical ensemble) for systems in the 2D Ising universality class,[11,19] namely $U^*_{CE} \sim 0.61$, indicating possible systematic errors in the second significant figure due to the correlations related to the decay of magnetic fluctuations; one needs to choose $n_0 \sim L^2$, and do longer runs, yielding

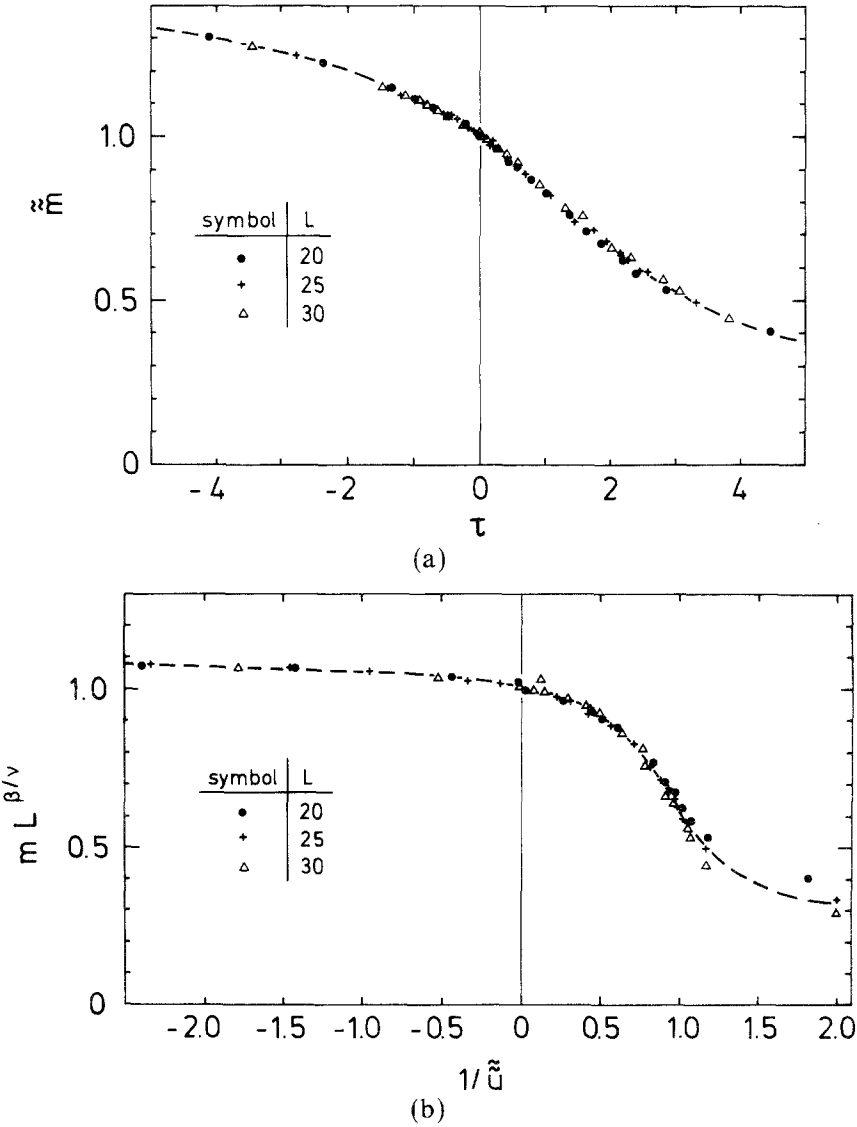

Fig. 6. (a) The scaled magnetization $\tilde{m}$ as a function of τ, the scaled temperature. (b) $\tilde{m}$ as a function of $1/\tilde{u}$ the reciprocal of scaled internal energy.

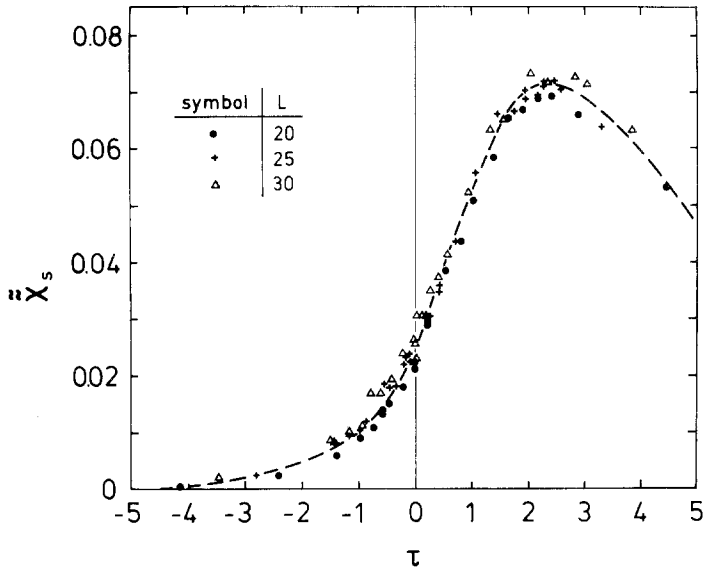

(a)

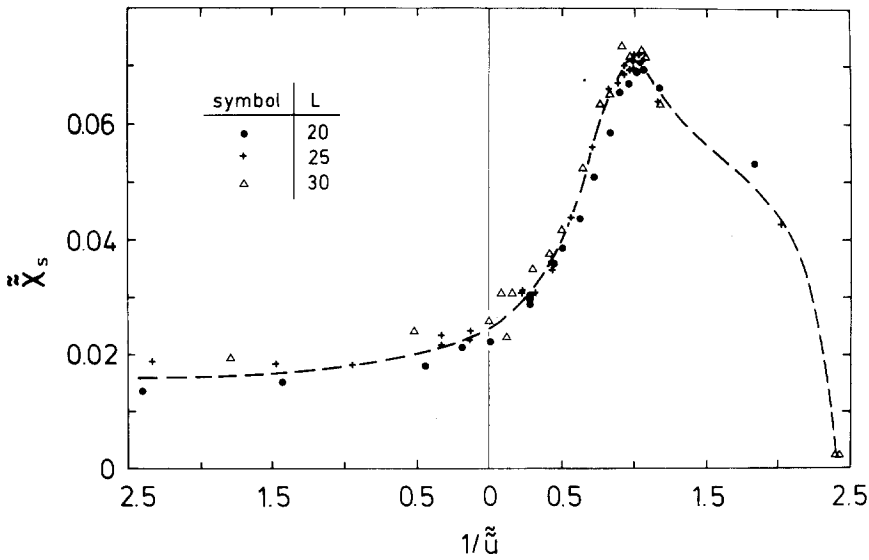

(b)

Fig. 7. (a) The scaled susceptibility $\tilde{\chi}_s$ as a function of τ, the scaled temperature. (b) $\tilde{\chi}_s$ as a function of $1/\tilde{u}$ the reciprocal of scaled internal energy.

better averaging. Since finite-size effects differ in different ensembles, we suspect that the difference between U^*_{MCE} and U^*_{CE} is a real effect and not an artifact of corrections to finite-size scaling. In Fig. 5a, we show the universal function $U(\tau)$ and in Fig. 5b, the corresponding universal function $U(1/\tilde{u})$. In Fig. 6a, similarly, we show the scaled magnetization $\tilde{m}$ as a function of τ and in Fig. 6b as a function of $1/\tilde{u}$. Finally, in Fig. 7a, we give $\tilde{\chi}_s$ with respect to τ and in Fig. 7b, with respect to $1/\tilde{u}$. Within the scatter of the data the scaling described in Section 2 appears to be obeyed. [in obtaining the scaled functions in Figs. 5b, 6b, and 7b, we have used the noncritical point $(T_0, u_0) = (2.817, -0.9)$, where $u_0 = u(T_0)$.]

4. SUMMARY

In this paper, we have extended the technique of finite-size scaling[8–11] to systems appropriate to a microcanonical ensemble. Recent simulation

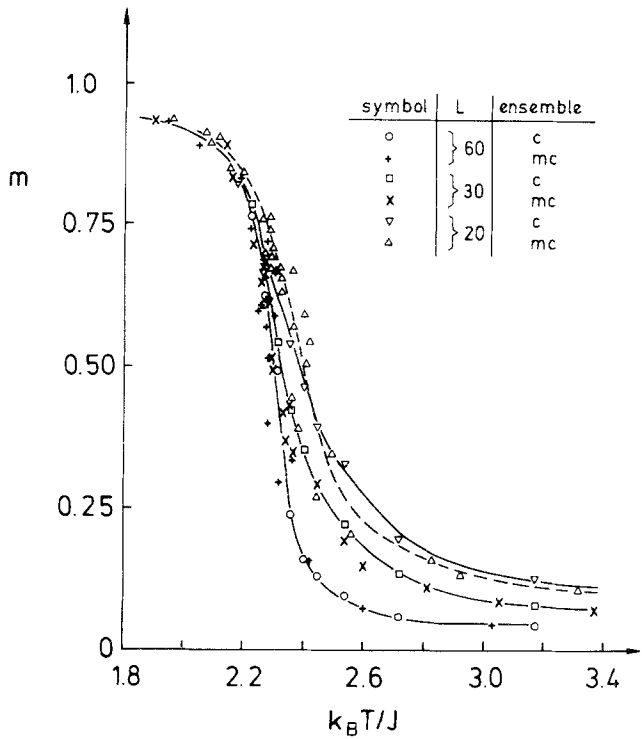

Fig. 8. Absolute value of the magnetization plotted versus temperature for three system sizes in the canonical ensemble (c) and in the microcanonical ensemble (mc). Canonical ensemble data are due to Landau.[20] Full and broken curves are guides to the eye only: full curves are drawn through the canonical ensemble data, while the broken curve is drawn through the microcanonical results for $L = 20$.

algorithms[2,6] which use deterministic Ising dynamics correspond to the microcanonical ensemble. Using one of them,[2] we have simulated an Ising square lattice system on a multitransputer system and demonstrated how the finite-size scaling method could be applied to microcanonical ensemble systems.

One rather basic question is not yet finally answered by the present work: What is the nature of the difference between finite-size effects in different ensembles? Suppose we take our present results for magnetization $m(u, L)$ and $T = T(u, L)$ to eliminate u in favor of T to construct a function $m(u(T, L), h) = m'(T, L)$ in the microcanonical ensemble: there is no reason, in our opinion, to expect *a priori* that $m'(T, L)$ agrees quantiatively with $m(T, L)$, the magnetization calculated in the canonical ensemble. Unfortunately, a comparison of the present data for $m'(T, L)$ with literature data[15] for $m(T, L)$ shows that the differences between m and m' hardly exceed the statistical errors; see Fig. 8. As indicated for $L = 20$ by the dashed curve, $m'(T, L)$ seems to vary a little bit steeper than $m(T, L)$ (full curve), but both curves intersect each other close to their inflection points, and there the systematic differences are hard to resolve accurately. This problem should be studied further by future high-precision work.

ACKNOWLEDGMENTS

One of us (R.C.D.) would like to thank the members of the Condensed Matter Theory Group at the University of Mainz for their hospitality during his stay. We gratefully acknowledge the support from the Sonderforschungsbereich 41.

REFERENCES

1. K. Binder, ed., *Applications of the Monte Carlo Method in Statistical Physics*, 2nd ed. (Springer, 1987).
2. M. Creutz, *Phys. Rev. Lett.* **50**:1411 (1983); see also D. Callaway and A. Rahman, *Phys. Rev. Lett.* **49**:613 (1982).
3. R. Harris, *Phys. Lett.* **111A**:299 (1985).
4. G. Bhanot, M. Creutz, and H. Neuberger, *Nucl. Phys. B* **235**[FS 11]:417 (1984).
5. D. W. Heermann, *Computer Simulation Methods in Theoretical Physics* (Springer, 1986); K. Binder and D. W. Heermann, *The Monte Carlo Method in Statistical Physics: An Introduction* (Springer, 1988).
6. H. J. Herrmann, *J. Stat. Phys.* **45**:145 (1986), and references therein.
7. R. C. Desai and D. Stauffer, *J. Phys. A. Math. Gen.* **21**:Lxxx (1988) and references therein.
8. M. N. Barber, in *Phase Transitions and Critical Phenomena*, Vol. 8, C. Domb and J. L. Lebowitz, eds. (Academic Press, New York, 1983), Chapter 2, p. 146.
9. M. E. Fisher, in *Critical Phenomena*, M. S. Green, ed. (Academic Press, New York, 1971), p. 1.

10. K. Binder, *Z. Phys. B* **43**:119 (1981).
11. K. Binder, *Ferroelectrics* **73**:43 (1987).
12. A. E. Ferdinand and M. E. Fisher, *Phys. Rev.* **185**:832 (1969).
13. C. Domb, *Adv. Phys.* **9**:149 (1960).
14. B. M. McCoy and T. T. Wu, *The Two-Dimensional Ising Model* (Harvard University Press, 1973).
15. D. P. Landau, *Phys. Rev. B* **13**:2997 (1976).
16. H. E. Stanley, *Phase Transitions and Critical Phenomena* (Oxford, 1971).
17. F. J. Wegner, *Phys. Rev. B* **5**:4529 (1972); F. J. Wegner and E. K. Riedel, *Phys. Rev. B* **7**:248 (1973).
18. D. W. Heermann and R. C. Desai, *Comput. Phys. Commun.* **50**:297 (1988).
19. A. Milchev, D. W. Heermann, and K. Binder, *J. Stat. Phys.* **44**:749 (1986).
20. D. P. Landau, *Phys. Rev. B* **13**:2996 (1976).